

Accepted Manuscript

Title: Preparation, characterisation and buccal permeation of naratriptan

Author: Mohammed Sattar Jonathan Hadgraft Majella E. Lane



PII: S0378-5173(15)30054-5
DOI: <http://dx.doi.org/doi:10.1016/j.ijpharm.2015.07.035>
Reference: IJP 15039

To appear in: *International Journal of Pharmaceutics*

Received date: 19-5-2015
Revised date: 11-7-2015
Accepted date: 13-7-2015

Please cite this article as: Sattar, Mohammed, Hadgraft, Jonathan, Lane, Majella E., Preparation, characterisation and buccal permeation of naratriptan. *International Journal of Pharmaceutics* <http://dx.doi.org/10.1016/j.ijpharm.2015.07.035>

This is a PDF file of an unedited manuscript that has been accepted for publication. As a service to our customers we are providing this early version of the manuscript. The manuscript will undergo copyediting, typesetting, and review of the resulting proof before it is published in its final form. Please note that during the production process errors may be discovered which could affect the content, and all legal disclaimers that apply to the journal pertain.

Preparation, characterisation and buccal permeation of naratriptan**Mohammed Sattar^{1,2}, Jonathan Hadgraft¹, Majella E. Lane¹**¹Department of Pharmaceutics

UCL School of Pharmacy

29-39 Brunswick Square

London

WC1N 1AX

United Kingdom

²Department of Pharmaceutics

College of Pharmacy

University of Basrah

Basrah

Iraq

*Corresponding author

Tel: +44 207 7535821

Fax: +44 870 1659275

Email: majella.lane@btinternet.com

Abstract

Naratriptan (NAR) is currently used for the management of migraine as the hydrochloride salt (NAR.HCl) and is administered as an oral tablet. This work evaluates the feasibility of buccal delivery of NAR in order to ensure faster onset of action and avoid the side-effects associated with conventional oral formulations. We hypothesised that the unionised form of NAR would permeate buccal tissue to a greater extent than the salt. Therefore the first stage of this work required preparation of the free base from NAR.HCl. Characterisation of the base with thermal and elemental analyses confirmed its purity; Log P and Log D values were also determined. The pH permeation profile of NAR was also

determined in the range 7.4 – 10. Solubility studies in non-aqueous solvents indicated that Transcutol™ (TC) and dipropylene glycol (DPG) were suitable vehicles for the free base. Maximum amounts of NAR which permeated after 6 h were $\sim 130 \mu\text{g}/\text{cm}^2$. Based on the pH permeation results and studies conducted at two different doses NAR appears to permeate porcine buccal tissue via the transcellular route. Finally, estimates of likely systemic values suggest that optimised formulations should be taken forward for *in vivo* evaluation.

Key words: Naratriptan, salt, base, buccal, pH, permeation

1. Introduction

Naratriptan (NAR), a 5-hydroxy tryptamine agonist, is used in the treatment of acute phase migraine as the hydrochloride salt (NAR.HCl). The drug is administered orally as a conventional tablet (1). Unfortunately, formulations currently available are not associated with good patient compliance because of related gastrointestinal adverse reactions (2). Buccal drug delivery (BDD) may offer an alternative route for administration of NAR with minimal side effects. This requires the active to permeate through the buccal epithelium in sufficient amounts to achieve effective therapeutic plasma concentrations. Orally disintegrating tablets of NAR.HCl were prepared and characterised by Stange et al. (3). However the ability of these preparations to deliver the drug across buccal tissue was not evaluated.

The penetration of a molecule through the hydrophilic and lipophilic domains of the buccal tissue depends largely on its physicochemical properties (4,5). Molecules, which are administered transdermally, have also been developed as commercial oral transmucosal preparations (6). This suggests that the desirable properties for buccal delivery are similar to those for drugs delivered transdermally for systemic effects. Typically these include low melting point, molecular weight (MW) < 500 and balanced log P values (7). Ionisation will also influence permeation; greater transmucosal permeation has been observed for the

unionised forms of a number of actives compared with their salts (8-10). Holm et al. (11) demonstrated pH-dependent permeation for metoprolol both *in vitro* and *in vivo* using porcine models with greater permeation at higher buffer pH values.

The aims of the present work were therefore to:

- (i) Prepare and characterise NAR base from the salt form.
- (ii) Determine the solubility and stability of NAR in a range of candidate vehicles.
- (iii) Compare the buccal permeation characteristics of the base with the salt using an *in vitro* porcine buccal model.

2. Materials and Methods

2.1 Materials

NAR HCl was obtained from Bioprogress (March, UK). Ethanol (ET), 99.7–100% (v/v) AnalaR[®] grade was supplied by VWR (UK). Transcutol P[®] (TC), Labrafac PG[®], Labrafac WL[®] and propylene glycol monolaurate (PGML) were gifts from Gattefossé (St. Priest, France). Oleic acid (OA) and polyethylene glycol 400 (PEG 400) were purchased from Fluka (Germany). Dipropylene glycol (DPG) and n-octanol were purchased from Acros Organics (USA). Miglyol[®] 812 N (MG) was obtained from Sasol (Germany). Isopropyl myristate (IPM) and isopropyl palmitate (IPP) were obtained from Croda Ltd (UK). Ethyl acetate, sodium hydroxide (NaOH) and Krebs-Ringer bicarbonate buffer (KRB) were obtained from Sigma-Aldrich (Germany). Polyethylene glycol 200 (PEG 200), propylene glycol (PG), phosphate buffered saline (PBS), HPLC grade acetonitrile (ACN), trifluoroacetate (TFA) and water were all obtained from Fisher Scientific (UK). Porcine buccal tissue was obtained from a local abattoir immediately after slaughter and transported

on ice. Caffeine (50 µg/ml in KRB) was used as a marker molecule to evaluate the integrity of the buccal tissue and permeation was monitored up to 6 h.

2.2 *Preparation of NAR base*

NAR.HCl was converted to the base form (Figure 1) by a simple acid-base reaction. NaOH (0.1M) was added slowly to an aqueous solution of the salt with gradual mixing. The precipitate was then removed by filtration (Whatman grade filter paper No.52, UK) and washed with distilled water. Two methods were used to collect the precipitate: (i) Drying over silica gel in a desiccator for 2 days at room temperature, or (ii) Dissolution in ethyl acetate and incubation overnight at 40°C to recrystallise the base. The final products were stored in airtight containers at 5°C.

2.3 *Thermogravimetric analysis (TGA) and Differential scanning calorimetry (DSC)*

Thermogravimetric analysis (TGA, Hi-Res 2950, TA Instruments, USA) was used to monitor the mass changes of the salt and base as a function of increasing temperature. This was performed in open aluminum hermetic pans with a heating rate of 10°C/min, from 35 - 300°C. Differential Scanning Calorimetry (DSC, Q2000, TA instruments, USA) was used to determine the melting point and purity of the salt and base. The DSC was calibrated using indium with a heating rate of 10°C/min over the temperature range from 35 - 275°C under dry nitrogen purging (50 mL/min) using hermetically sealed pans.

2.4 *Elemental analysis and Liquid Chromatography Mass Spectrometry (LC-MS)*

The salt and the base were analysed to determine the carbon, hydrogen and nitrogen content using an Elemental Analyser (Carlo-Erba, EA 1108, Italy). LCMS (Alliance 2695 Separations module with Micro mass ZQ Mass Detector 2996 Photodiode Array Detector,

Waters, Ireland) was used to determine the purity of both species when dissolved in methanol. The chromatographic column was an Onyx™ Monolithic C₁₈, LC Column (50 x 4.6 mm). The volume of injection was 10 µL and the column was maintained at 35°C. The flow rate was 1.5 mL/min, and the run time was 10 min. A gradient method was used for analysis with the mobile phase consisting of 0.1% formic acid in water and acetonitrile.

2.5 High Performance Liquid Chromatographic (HPLC) analysis

A stock solution of 100 µg/mL of NAR in water was used to prepare a series of concentrations ranging from 0.5 - 30 µg/mL. These standards were used to construct a calibration curve for HPLC analysis (Agilent 1100, USA operated with ChemStation® software). A Phenomenex PhenoSphere™ CN 80 Å (250 × 4.6 mm, 5 µm) fitted with a C₁₈ cartridge (20 × 4.6 mm, 5µm) was used for analysis. Ultraviolet (UV) detection at 284 nm was employed; the injection volume was 10 µL and the column temperature was maintained at 40°C. The mobile phase solution consisted of 0.1% TFA in water with ACN (78:22, v/v). The flow rate was 1 mL/min, and the run time was 8 min. Under these conditions, NAR exhibited a retention time of 5.4 ± 0.1 min. The HPLC method was validated in terms of specificity, linearity, accuracy, precision, detection limit and quantification limit according to International Conference of Harmonization guidelines (12). The limit of detection was 0.23 µg/mL while the limit of quantification was 0.7 µg/mL.

2.6 Solubility studies, solubility parameter and stability

For solubility determination in candidate vehicles an excess amount of NAR was added to one mL of solvent in a reaction tube and sonicated for five minutes. The suspensions were kept at 37°C for 2 days with continuous rotation. Thereafter, the tubes were centrifuged and 50 µL of the clear supernatant was diluted and quantified by HPLC. Experiments were

performed in triplicate and mean values with standard deviations (SD) were calculated (13,14). To determine solubility at different pH values, excess NAR was added to PBS to which a few drops of 0.1M HCl or 0.1M NaOH were added to obtain the required pH value. Suspensions were stirred for 48 h at room temperature. The pH was measured using a SympHony™ pH meter (SB70P, VWR, Germany) and corrected with 0.1M HCl or 0.1M NaOH to the required pH value at 24 and 48 h. Suspensions were centrifuged for 15 min at 13200 rpm. Finally, the supernatant was diluted and quantified by HPLC. Experiments were performed in triplicate and mean values with SD were calculated. The relative composition of each NAR micro-species in solution as a function of pH was calculated using Equations 1 – 3 (15).

$$NAR^+ = \frac{[H^+]^2}{[H^+]^2 + K_{a1}[H^+] + K_{a1}K_{a2}} \quad \text{Equation 1}$$

$$NAR = \frac{K_{a1}[H^+]}{[H^+]^2 + K_{a1}[H^+] + K_{a1}K_{a2}} \quad \text{Equation 2}$$

$$NAR^- = \frac{K_{a1}K_{a2}}{[H^+]^2 + K_{a1}[H^+] + K_{a1}K_{a2}} \quad \text{Equation 3}$$

Where NAR^+ , NAR , NAR^- are NAR micro species, $[H^+]$ is hydrogen ion concentration, and K_{a1} , K_{a2} are the dissociation constants.

The short term stability of NAR in various solvents was determined by preparing solutions with concentrations equal to 30% of their original solubility. The solutions were kept at 37°C for 3 days with continuous rotation and samples were analysed by HPLC at time

zero and at 24 h intervals. The percentage of NAR remaining versus time was determined. The study was conducted in triplicate. The three dimensional solubility parameters (δ) of the drug and vehicles were calculated according to the Van Krevelen 3-D approach utilising Molecular Modeling Pro[®] software (Chem SW, Inc., USA).

2.7. Determination of partition ($\log P$) and distribution coefficients ($\log D$)

For the determination of $\log P$, octanol pre-saturated with water and water pre-saturated with octanol was achieved by mixing 50 mL of each solvent in a conical flask, followed by stirring for 48 h. A modification of the method reported by Birudaraj et al. (10) was used to measure $\log D$ and octanol was saturated with the PBS adjusted as described in the previous section. A stock solution of 0.1 mg/mL of NAR in the saturated octanol layer was prepared and mixed with the saturated aqueous layer; three different ratios of octanol:water or pH adjusted PBS were studied (1:1, 1:2, 2:1). Tubes were agitated 100 times over 5 min and allowed to stand for 48 h (16). A sample from each phase was diluted and analysed by HPLC. The log of the partition coefficient or distribution coefficient was calculated using the relative NAR concentrations in n-octanol / water or n-octanol / pH adjusted PBS. All measurements were conducted at room temperature and in triplicate.

2.8 *In vitro* permeation experiments

Porcine buccal tissue was obtained from a local abattoir immediately after slaughter and was transported on ice. All experiments were conducted with fresh tissue. The buccal mucosa was separated from the underlying tissues with surgical scissors and a scalpel blade. The mucosa was trimmed using a dermatome to a thickness of 0.8 ± 0.1 mm. Tissue was cut to suitable dimensions and mounted in Franz diffusion cells. The diffusional area was ~ 1 cm² (the diameters for each cell were measured accurately). Approximately 5 ml of PBS (pH 7.4)

was used as the receptor phase after degassing with high speed stirring under a vacuum for 20 min in a Nuova II stirrer (Thermolyne, USA) connected to a vacuum pump. Cells were placed in a water bath set at 37°C and 1 mL of PBS was added to the donor chamber for 30 min to ensure tissue hydration and to mimic as best as possible the conditions in the mouth. The temperature of the cells was routinely measured with a thermometer (Corby, UK) until all cells were at $37 \pm 0.5^\circ\text{C}$. Donor PBS was removed immediately before the addition of any formulations. The test solution (100 μL) was then added to the donor chamber. Permeation experiments were conducted under occlusion by covering the donor compartments with ParafilmTM. A volume of 200 μL was withdrawn from each receptor chamber at specific time intervals and replaced with an equal volume of warm fresh degassed PBS. Three to five experiments were conducted for each formulation. NAR.HCl was dissolved in water, PG, TC, PEG 200, or PEG 400 at a concentration of 2.5 mg/mL and 1 mL was applied to the donor chamber. NAR was dissolved in TC and DPG at concentrations of 2.5 mg/mL and 25 mg/mL (as the current therapeutic dose is 2.5 mg) to study the effect of dose on NAR buccal delivery; 100 μL was applied in the donor chamber. To study the influence of pH on NAR buccal delivery, the donor chamber was charged with 1 mL of saturated drug solution in PBS (pH= 7.4, 8.5, 9.5, and 10). The cumulative amount of drug permeated per unit area of buccal mucosa ($\mu\text{g}/\text{cm}^2$) was plotted against the collection time (6 h) and reported as Q_{6h} ; the slope of this graph at the steady state was considered as the flux (J_{ss}) and the extrapolated x-axis intercept as the lag time (t_{lag}). The permeability coefficient (k_p) was determined as reported previously (17).

Mass balance studies were conducted to quantify the amount of drug in the different compartments of the Franz cells as well as in the tissue. Initially, the remaining amount of formulation on the tissue was pipetted out, diluted and analysed using HPLC. Secondly, the surface of the membrane was washed three times sequentially with 1 mL of methanol:water

(50:50, v/v). Finally, the cells were disassembled and the buccal membranes were cut into small pieces and incubated in 5 mL of methanol:water (50:50, v/v) at 37°C with 12 h of shaking in order to extract any remaining drug inside the tissue. Buccal washes and extracts were centrifuged for 20 min at 13.2 ($\times 1000$) rpm (Eppendorf centrifuge, UK) and a sample of the supernatant was diluted and analysed by the HPLC. The final cumulative amount of drug permeated was used to calculate the recovery of the drug in the receptor phase. Validation of the washing and extraction procedure was conducted and results confirmed $97.5 \pm 1.4\%$ recovery of the applied active for the washing procedure and 96% recovery for the extraction step.

2.9 Statistical analysis

The data were analysed using a software package (SPSS version 22) and Excel (Microsoft Office 2010). All results are presented as mean \pm standard deviation (SD). The Student's *t*-test and one-way analysis of variance (ANOVA) with replication using the Post Hoc Tukey test were used to investigate statistical differences. A probability of $p < 0.05$ was considered statistically significant.

3. Results and Discussion

3.1 Thermal, elemental and LC-MS analyses

The molecular weight and the melting point for NAR (Figure 1) are 335.4 g/mole and 170° to 171°C and the corresponding values for NAR.HCl are 371.9 g/mole and 237° to 239° C, respectively (18). NAR base prepared following drying had the appearance of a white powder. Visual inspection suggested that the precipitate collected after dissolution in ethyl acetate and evaporation was crystalline. The percentage yield of the resultant precipitate was $78 \pm 5\%$, with some of the drug likely being lost during the washing steps. Figure 2 shows the thermograms for the salt and the base prepared from aqueous solution or from ethyl

acetate. The precipitate recrystallised from ethyl acetate shows a thermal curve similar to that for the salt with a gradual slope around 170°C (near the melting point of NAR base). However the thermogram of the base prepared without ethyl acetate indicates the presence of some residual water molecules in the sample. DSC analysis was consistent with the TGA results. Figure 3 shows the DSC scan for the salt and the base prepared from ethyl acetate. The melting point for NAR.HCl is 248°C and this peak was absent in the thermogram of the base, which clearly indicated the complete conversion of the salt to the base. The presence of a single endothermic sharp peak confirmed that the entire drug was converted to a form with a melting point of 178°C. CHN analysis indicated good agreement between the practical and theoretical mass fractions of C, H and N atoms in NAR.HCl, and in the base prepared from ethyl acetate. A single peak was obtained for the LCMS analysis confirming the purity of the sample. This sample was used in all subsequent studies because of the residual water in the product recrystallised from the aqueous solution.

3.2 Solubility, solubility parameter and stability results

Solubility and stability studies were conducted in a range of solvents commonly used in topical and transdermal preparations (Figure 4). NAR was noted to be stable in all the tested solvents when incubated at 37°C for 3 days. The solubility parameter (δ) of NAR was calculated to be 12.52 (cal/cm³)^{0.5}. NAR shows the highest solubility in TC which has a δ value of 10.62 (cal/cm³)^{0.5}. High solubility was also observed in DPG, ET and PEG 200 with corresponding δ values of 12.19, 12.26 and 12.06 (cal/cm³)^{0.5}. Lowest solubility was observed for the solvents with δ values in the range of 7-9 (cal/cm³)^{0.5} which included MG, IPM, IPP, Labrafac PG[®] and Labrafac WL[®], with the exception of OA. The higher solubility in OA may reflect association of the positive charge of the tertiary amine group of NAR and the carboxylic acid moiety of OA. The maximum solubility of NAR.HCl was determined in

water (27.3 ± 0.5 mg/mL) followed by PG (14.9 ± 0.4 mg/mL), PEG 200 (10.9 ± 0.6 mg/mL), PEG 400 (3.1 ± 0.1 mg/mL) and TC (1.0 ± 0.1 mg/mL).

3.3 Partition and distribution coefficients

The average log P of NAR for the three octanol:water ratios investigated was determined to be 0.63 ± 0.08 with a total drug recovery of $96.7\% \pm 1.7$. NAR has two different pK_a values as a result of (i) A basic piperidine ring - pK_a 9.6, and (ii) An acidic sulfamide group - pK_a 10.6. At pH 10 around 60% of NAR is present in the unionised form and the drug shows the highest log D and lowest solubility, while at physiological pH (6.8 to 7.4) the situation is reversed. Figure 5 shows the change in Log D value as a function of pH with solubility values of NAR ranging from 16.8 mg/ml at pH 7.4 to 0.3 mg/ml at pH 10.

3.4 In vitro permeation studies

Single solvents

Permeation studies conducted with caffeine confirmed the integrity of all tissues (data not shown). No permeation of NAR.HCl was observed from an aqueous solution (2.5 mg/mL) and at the same concentrations in PG, PEG 200, PEG 400 and TC. The results of the mass-balance studies for PG, PEG 200, PEG 400 and TC confirmed that more than 95% of the applied doses of NAR.HCl were recovered from the membrane surface and less than 2% was extracted from the tissue. The extracted amount of NAR.HCl for the various solvents may be ranked as follows: PG > TC > PEG 200 > PEG 400.

Permeation studies for NAR were conducted in the two solvents for which NAR exhibited the highest solubility. The permeation profiles for two concentrations of NAR in TC and DPG (2.5 mg/ml and 25 mg/ml) across porcine buccal mucosa over 6 h are shown in Figure 6; permeation parameters are summarised in Table 1. Lag times (t_{lag}) ranged from 165

to 213 min and are comparable to values reported for other studies with porcine buccal tissue (19). However, the thickness of the tissue will also influence the magnitude of this parameter (20). Steady state flux and cumulative permeation values were significantly higher ($p < 0.05$) for NAR in TC compared with NAR in DPG for both doses investigated. TC (diethylene glycol monomethyl ether) is used in the formulation of cosmetics and pharmaceuticals and manufacture of food additives because of its excellent solvent properties (21). It is also used as a skin penetration enhancer (22). Similarly, DPG is used in both cosmetic and pharmaceutical products for its solvent and humectant capabilities (22) but only limited data are available for its use or administration via the oral route. NAR permeated in a concentration-dependent manner from both solvents as the flux values and the cumulative amount permeated increased proportionally with the dose (Figure 6, Table 1). These findings are consistent with NAR permeation across the buccal mucosa being a passive diffusion process.

pH permeation studies

To understand the influence of pH on NAR buccal delivery, the permeability was determined in phosphate buffer saline (PBS) in the pH range 7.4 - 10. This range was selected to encompass the pK_a value associated with the piperidine ring of NAR (9.6). The permeation profiles (expressed as percentage of applied dose) over 8 h following application of 1 mL of saturated solutions of NAR are shown in Figure 7. Figure 7 clearly shows that solutions with a higher pH value resulted in a higher percentage of tissue penetration with more rapid permeation across the buccal mucosa. The percentage permeation of NAR for the pH 10 solution was significantly greater than for solutions with lower pH values (ANOVA, $p < 0.05$). Results for mass balance studies are shown in Figure 8. The permeation profiles are consistent with the mass balance studies where the amount of NAR deposited in the buccal

membrane was also pH-dependent. The increase in drug-tissue content at higher pH values is consistent with the increase in the distribution coefficient. Table 2 summarises NAR permeability coefficients, percentages permeated over 8 h, unionised fractions and distribution coefficients for the pH range studied. Although tissue integrity was not evaluated at the end of these permeation experiments, other researchers report no epithelial changes for experiments conducted with excised porcine tissue in the pH range 7.4 – 9.0 (23). These authors also reported no significant differences in lag times for mannitol permeation for studies conducted at pH 7.4 compared with pH 9.0; surprisingly, lag times for studies conducted at pH 8.5 were significantly longer than for pH 7.4.

The permeability coefficient (k_p) of NAR increased significantly (ANOVA, $p < 0.05$) with pH. A seven-fold increase in the buccal permeability coefficient and a ten-fold increase in the percentage of drug which permeated were observed over the pH range studied. The increase in the k_p values and the fraction of NAR permeated after 8 h at the higher pH values are in line with the increase of the fraction of unionised species and the calculated distribution coefficients. There are two major routes for drug permeation through the buccal mucosal membrane: paracellular and transcellular (24). It has also been suggested that if the drug is transported through the paracellular route (without partitioning), pH should not affect drug absorption rate. For the transcellular pathway the drug absorption rate is pH dependent.

Porcine buccal tissue has been used to model oral transmucosal delivery of a wide range of drug molecules *in vitro* (6). Histological features of porcine buccal tissue are reported to be similar to those of humans as well as its permeability to water (25,26). The influence of various experimental variables on drug permeation in such *ex vivo* models has also been studied extensively (20, 27-28). Recently, the relationship between drug permeation in *ex vivo* porcine and human buccal tissue models has also been explored (23). Although porcine tissue was approximately two-fold more permeable to metoprolol than human tissue a

good correlation between the two models was observed ($r^2=0.96$). Histomorphological examination also confirmed similar features for tissue from the two species.

The maximum amount of NAR which permeated after 6 h was $\sim 130 \mu\text{g}/\text{cm}^2$ when dosed at 25 mg/ml in Transcutol™ (100 μl application). The mean plasma concentration and clearance values of NAR following oral administration are reported as 8 $\mu\text{g}/\text{L}$ (ranging from 5.9-10.7 $\mu\text{g}/\text{L}$) and 6.6 mL/min/kg (18). Assuming a 70 kg patient and calculating NAR input from the flux values in Table 1, a plasma level of 1.8 $\mu\text{g}/\text{L}$ of NAR is possible from an area of application of 1 cm^2 . Although this falls below the mean therapeutic plasma values reported for humans, an application area of 4.4 cm^2 should theoretically result in a plasma concentration of 8 $\mu\text{g}/\text{L}$.

4. Conclusions

NAR was prepared and characterised from its hydrochloride salt; Log D and Log P values were also determined. Solubility and stability screening was conducted for a range of single solvents. Although no buccal permeation was observed for NAR.HCl this is the first report of buccal permeation of NAR. There is scope to optimise further these simple vehicles for buccal delivery which will be explored in a future paper. NAR permeated porcine buccal tissue in a concentration-dependent manner which suggests NAR permeates buccal mucosa via a passive diffusion process. Permeability experiments and mass balance studies showed that NAR permeated the buccal mucosa more favourably as the unionised form. The pH dependent permeability of NAR provides further support for the transcellular pathway being the primary route of transport of the molecule. Finally, differences in permeability characteristics of porcine and human buccal tissue are acknowledged however the *in vitro* porcine model appears to offer the closest alternative to studies with tissue from invasive biopsies in humans.

Acknowledgement

The Higher Committee for Education Development in Iraq is acknowledged for the provision of a studentship to support this work.

References

1. Martindale, 2014. Naratriptan HCl Monograph, The Complete Drug Reference. (Ed. A. Brayfield). Thirty-eight edition, London, Pharmaceutical Press.
2. BNF, 2014. Joint Formulary Committee. British National Formulary. 66th Ed. London, BMJ Group and Pharmaceutical Press.
3. Stange, U., Fuhrling, C., Gieseler, H., 2014. Formulation, preparation, and evaluation of novel orally disintegrating tablets containing taste-masked naproxen sodium granules and naratriptan hydrochloride. *J Pharm Sci* 103, 1233-1245.
4. Harris, D., Robinson, J.R., 1992. Drug delivery via the mucous membranes of the oral cavity. *J Pharm Sci* 81, 1-10.
5. Gandhi, R.B., Robinson, J.R., 1994. Oral cavity as a site for bioadhesive drug delivery. *Adv Drug Del Rev* 13, 43-74.
6. Sattar, M., Sayed, O.M., Lane, M.E., 2014. Oral transmucosal drug delivery – Current status and future prospects. *Int J Pharm* 471, 498-506.
7. Hadgraft, J., 2004. Skin deep. *Eur J Pharm Biopharm* 58, 291-299.
8. Nair, M.K., Chetty, D.J., Ho, H., Chien, Y.W., 1997. Biomembrane permeation of nicotine: mechanistic studies with porcine mucosae and skin. *J Pharm Sci* 86, 257-262.

9. Deneer, V.H., Drese, G.B., Roemele, P.E., Verhoef, J.C., Lie, A.H.L., Kingma, J.H., Brouwers, J.R., Junginger, H.E., 2002. Buccal transport of flecainide and sotalol: effect of a bile salt and ionization state. *Int J Pharm* 241, 127-134.
10. Birudaraj, R., Berner, B., Shen, S., Li, X., 2005. Buccal permeation of buspirone: mechanistic studies on transport pathways. *J Pharm Sci* 94, 70-78.
11. Holm, R., Meng-Lund, E., Andersen, M.B., Jespersen, M.L., Karlsson, J.J., Garmer, M., Jorgensen, E.B., Jacobsen, J., 2013. In vitro, ex vivo and in vivo examination of buccal absorption of metoprolol with varying pH in TR146 cell culture, porcine buccal mucosa and Gottingen minipigs. *Eur J Pharm Sci* 49, 117-124.
12. ICH, 2005. International conference on harmonization, Validation of analytical procedures: text and methodology Q2(R1) ICH Harmonised Tripartite Guideline, USA, pp. 1-13.
13. Dias, M., Hadgraft, J., Lane, M.E., 2007. Influence of membrane-solvent-solute interactions on solute permeation in model membranes. *Int J Pharm* 336, 108-114.
14. Oliveira, G., Hadgraft, J., Lane, M.E., 2012. The influence of volatile solvents on transport across model membranes and human skin. *Int J Pharm* 435, 38-49.
15. Holler, F.J., Crouch, S.R., 2013. Complex acid/base systems, Skoog and West's Fundamentals of analytical chemistry. Cengage Learning, Hampshire, pp. 348-380.
16. OECD, 1995. Guideline for the testing of chemicals, Partition Coefficient (n-octanol/water): Shake Flask Method, pp. 1-4.
17. Oliveira, G., Beezer, A.E., Hadgraft, J., Lane, M.E., 2010. Alcohol enhanced permeation in model membranes. Part I. Thermodynamic and kinetic analyses of membrane permeation. *Int J Pharm* 393, 61-67.
18. Moffat, A.C., Osselton, M.D., Widdop, B., Watts, J., 2004. Clarke's analysis of drugs and poisons. Volume 2, 4th ed. London, The Pharmaceutical Press, pp. 1320-1321.

19. Amores, S., Lauroba, J., Calpena, A., Colom, H., Gimeno, A., Domenech, J.. 2014. A comparative ex vivo drug permeation study of beta-blockers through porcine buccal mucosa. *Int J Pharm.* 468, 50-4.
20. Kulkarni, U., Mahalingam, R., Pather, S.I., Li, X., Jasti, B., 2009. Porcine buccal mucosa as an *in vitro* model: relative contribution of epithelium and connective tissue as permeability barriers. *J Pharm Sci* 98, 471-483.
21. Sullivan, D.W., Jr., Gad, S.C., Julien, M., 2014. A review of the nonclinical safety of Transcutol(R), a highly purified form of diethylene glycol monoethyl ether (DEGEE) used as a pharmaceutical excipient. *Food Chem Toxicol* 72, 40-50.
22. Lane, M.E., 2013. Skin penetration enhancers. *Int J Pharm* 447, 12-21.
23. Meng-Lund, E., Marxen, E., Pedersen, A.M.L., Müllertz, A., Hyrup, B., Holm, R., Jacobsen, J., 2014. Ex vivo correlation of the permeability of metoprolol across human and porcine buccal mucosa. *J Pharm Sci* 103, 2053-2061.
24. Wertz, P.W., Squier, C.A., 1991. Cellular and molecular basis of barrier function in oral epithelium. *Crit Rev Ther Drug Carrier Syst* 8, 237-269.
25. Heaney, T.G., Jones, R.S., 1978. Histological investigation of the influence of adult porcine alveolar mucosal connective tissues on epithelial differentiation. *Arch Oral Biol* 23, 713-717.
26. Lesch, C.A., Squier, C.A., Cruchley, A., Williams, D.M., Speight, P., 1989. The permeability of human oral mucosa and skin to water. *J Dent Res* 68, 1345-1349.
27. Nicolazzo, J.A., Reed, B.L., Finnin, B.C., 2003. The effect of various *in vitro* conditions on the permeability characteristics of the buccal mucosa. *J Pharm Sci* 92, 2399-2410.

28. Kulkarni, U., Mahalingam, R., Pather, I., Li, X., Jasti, B., 2010. Porcine buccal mucosa as *in vitro* model: effect of biological and experimental variables. J Pharm Sci 99, 1265-1277.

Table 1: NAR permeation parameters for *in vitro* permeation experiments in TC and DPG when dosed at 2.5 mg/mL and 25 mg/mL (n>3, mean±S.D.)

Table 2: NAR unionised fraction, Log D, k_p and percentage permeated after 8 h for saturated solutions of varying pH

Table 1: NAR permeation parameters for *in vitro* permeation experiments in TC and DPG when dosed at 2.5 mg/mL and 25 mg/mL (n>3, mean±S.D.)

| | TC | | DPG | |
|--|------------------|------------------|-------------------|------------------|
| | NAR 2.5 mg/mL | NAR 25 mg/ml | NAR 2.5 mg/mL | NAR 25 mg/ml |
| J_{ss} ($\mu\text{g}/\text{cm}^2/\text{min}$) | 0.09 ± 0.05 | 0.83 ± 0.39 | 0.022 ± 0.001 | 0.23 ± 0.01 |
| t_{lag} (min) | 207.7 ± 16.7 | 211.3 ± 12.3 | 164.9 ± 35.8 | 213.1 ± 16.4 |
| $k_p * 10^{-6}$ (cm/min) | 35.6 ± 20.8 | 33.4 ± 15.7 | 8.9 ± 3.8 | 9.2 ± 0.5 |
| Q_{6h} ($\mu\text{g}/\text{cm}^2$) | 13.5 ± 7.1 | 127.1 ± 60.2 | 4.4 ± 1.6 | 38.9 ± 5.5 |

Table 2: NAR unionised fraction, Log D, k_p and percentage permeated after 8 h for saturated solutions of varying pH

| pH | Unionised Fraction | Log D | k_p (cm/s) *10^7 | Percentage permeated (%) |
|-----------|---------------------------|------------------|---|---------------------------------|
| 7.4 | 0.8 | -0.15 ± 0.01 | 4.9 ± 1.4 | 2.7 ± 1.1 |
| 8.5 | 9.1 | 0.26 ± 0.02 | 9.6 ± 2.1 | 5.0 ± 1.1 |
| 9.5 | 48.1 | 0.67 ± 0.04 | 15.1 ± 5.8 | 9.3 ± 4.2 |
| 10 | 63.8 | 1.15 ± 0.09 | 34.2 ± 10.8 | 27.6 ± 5.1 |

LIST OF FIGURES

Figure 1: Chemical structure of NAR

Figure 2: TGA thermograms of NAR.HCl, base prepared from ethyl acetate and base prepared from aqueous solution

Figure 3: DSC thermogram of NAR.HCl and NAR recrystallised from ethyl acetate

Figure 4: Solubility of NAR in various solvents at 37°C (n= 3, Mean ± S.D.)

Figure 5: Log D of NAR as a function of pH

Figure 6: Cumulative amount ($\mu\text{g}/\text{cm}^2$) naratriptan permeated for 2.5 mg/mL or 25 mg/mL solutions in TC and DPG (n \geq 3, mean \pm SD)

Figure 7: Percentage of NAR permeation from saturated solutions of pH values 7.4 – 10 over 8 h (n=5, mean \pm SD) * denotes significant differences ($p < 0.05$)

Figure 8: NAR mass balance studies for permeation studies of saturated drug in PBS for the pH range 7.4 – 10 (n=5, mean \pm SD); * denotes significant differences ($p < 0.05$)

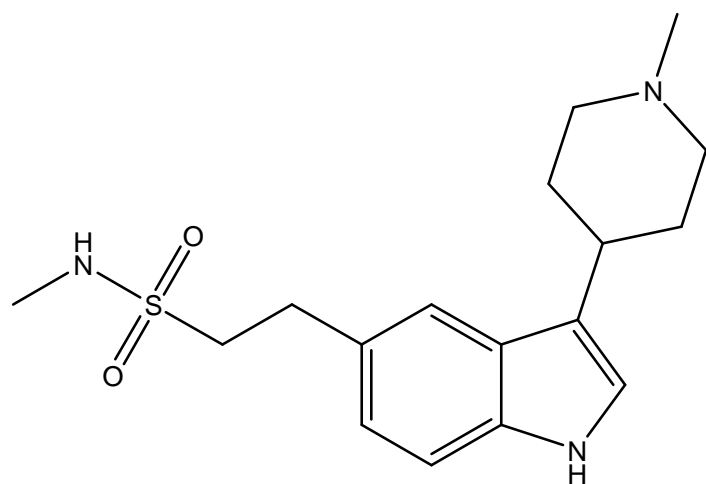


Figure 1: Chemical structure of NAR

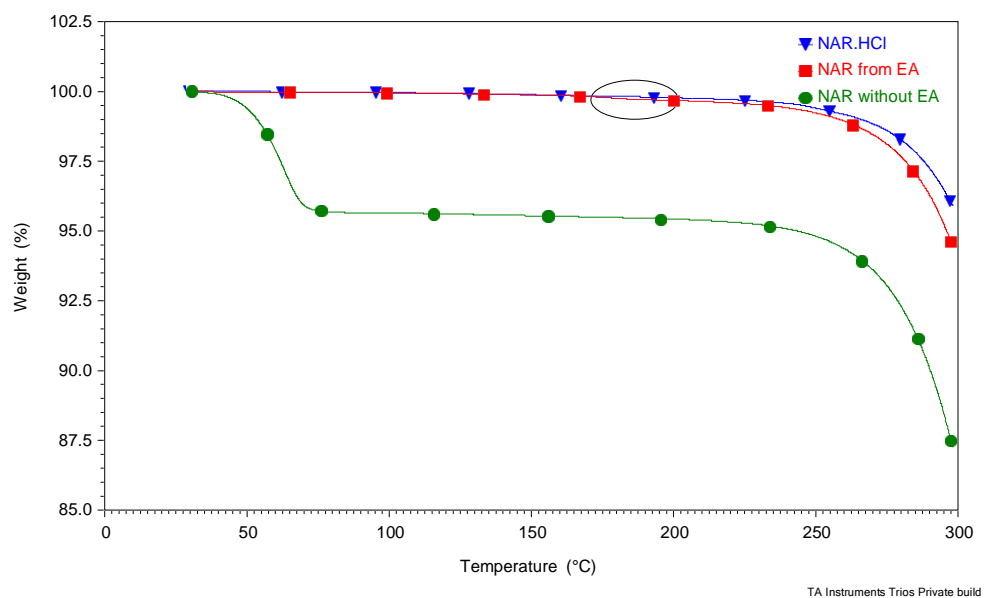


Figure 2: TGA thermograms of NAR.HCl, base prepared from ethyl acetate and base prepared from aqueous solution

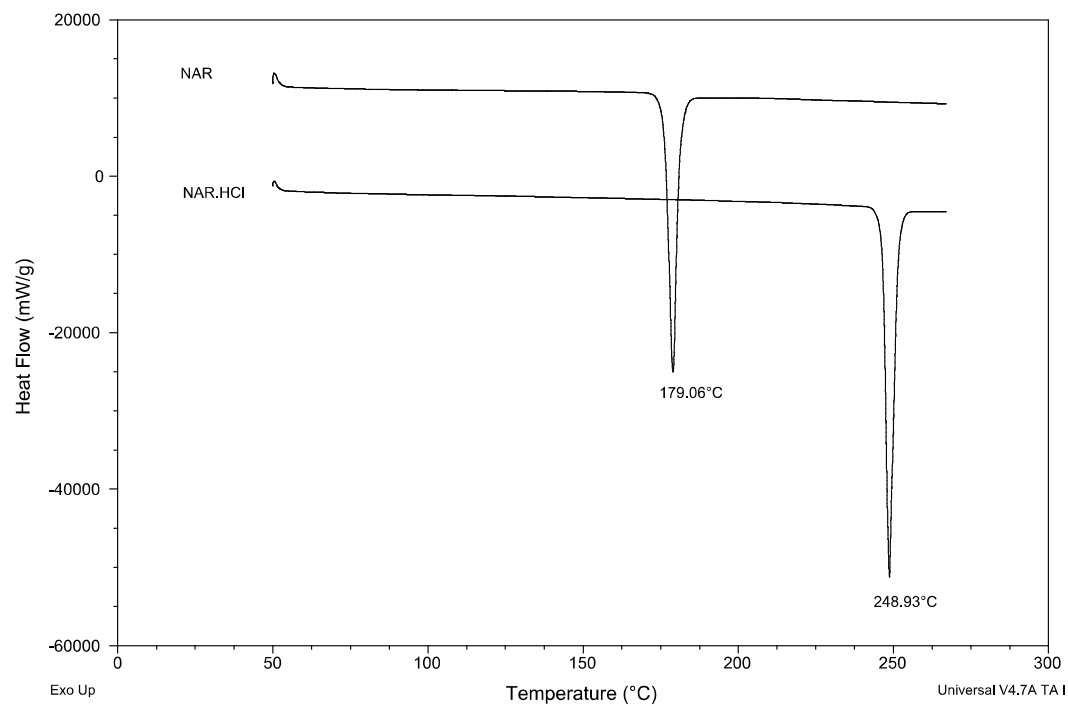


Figure 3: DSC thermogram of NAR.HCl and NAR recrystallised from ethyl acetate

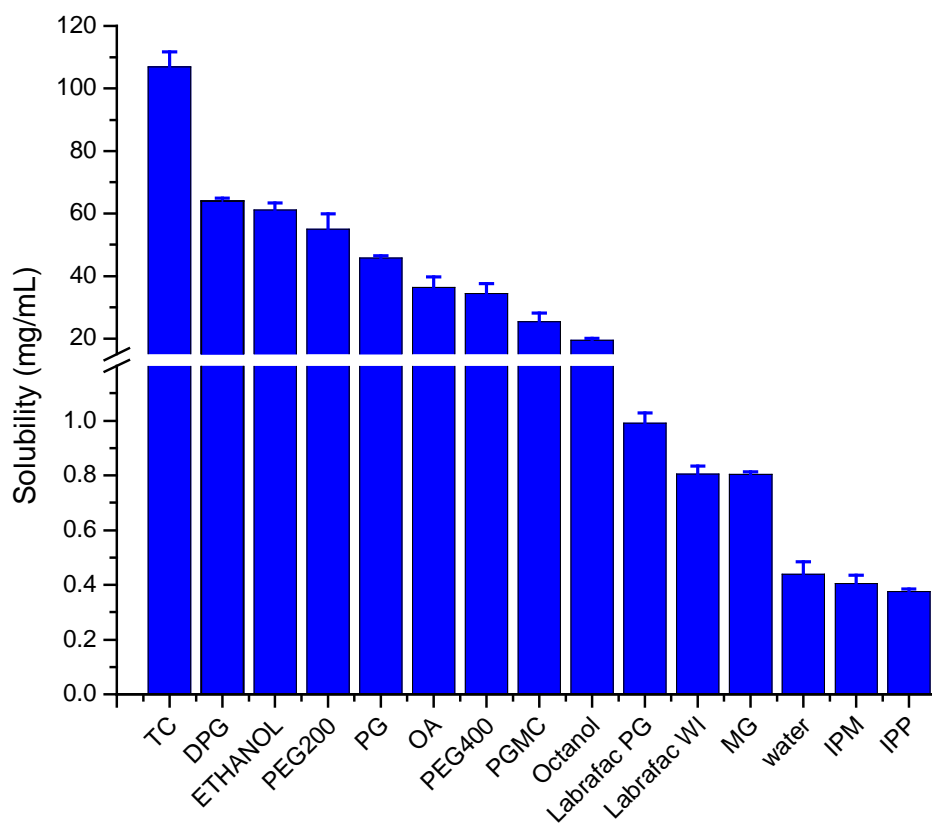


Figure 4: Solubility of NAR in various solvents at 37°C (n= 3, Mean \pm S.D.)

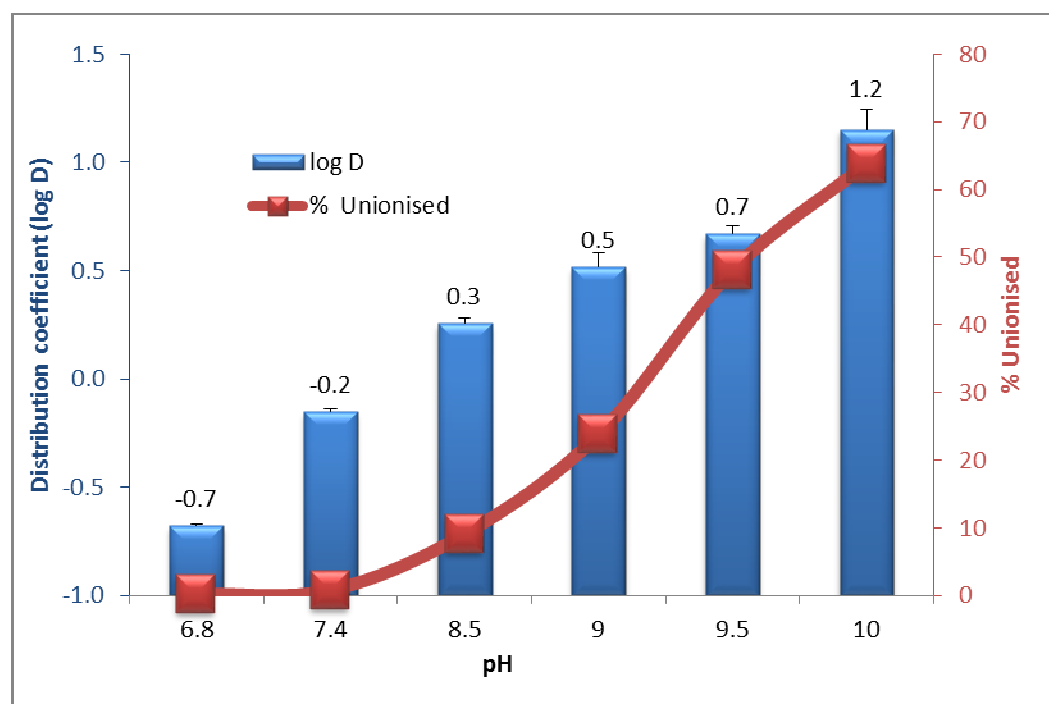


Figure 5: Log D of NAR as a function of pH

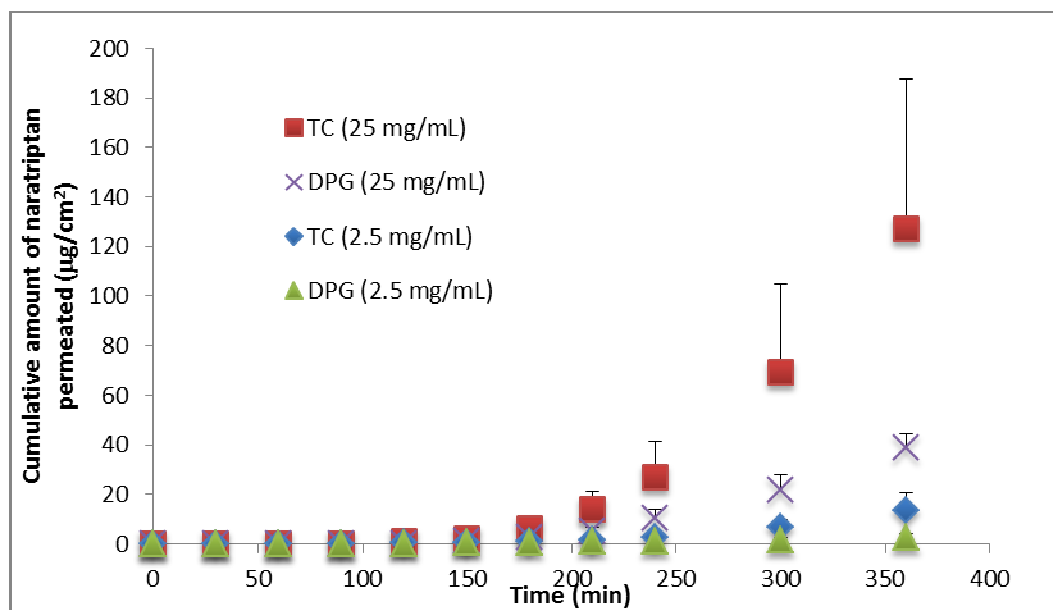


Figure 6: Cumulative amount ($\mu\text{g}/\text{cm}^2$) naratriptan permeated for 2.5 mg/mL or 25 mg/mL solutions in TC and DPG ($n \geq 3$, mean \pm SD)

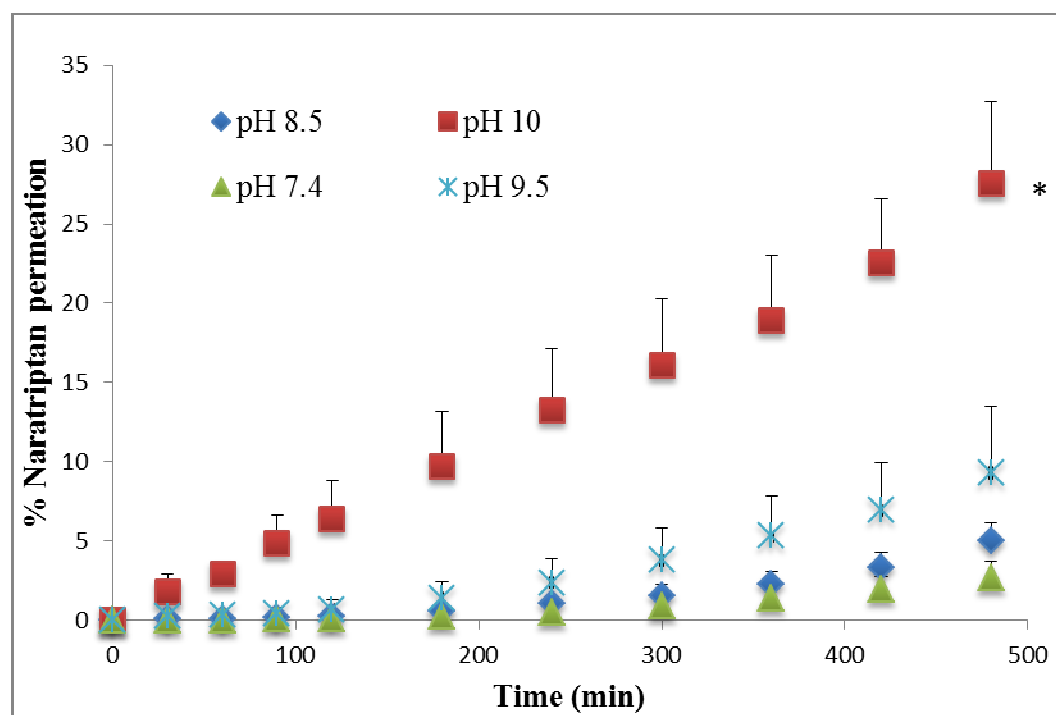


Figure 7. Percentage of NAR permeation from saturated solutions of pH values 7.4 – 10 over 8 h (n=5, mean± SD) * denotes significant differences ($p < 0.05$)

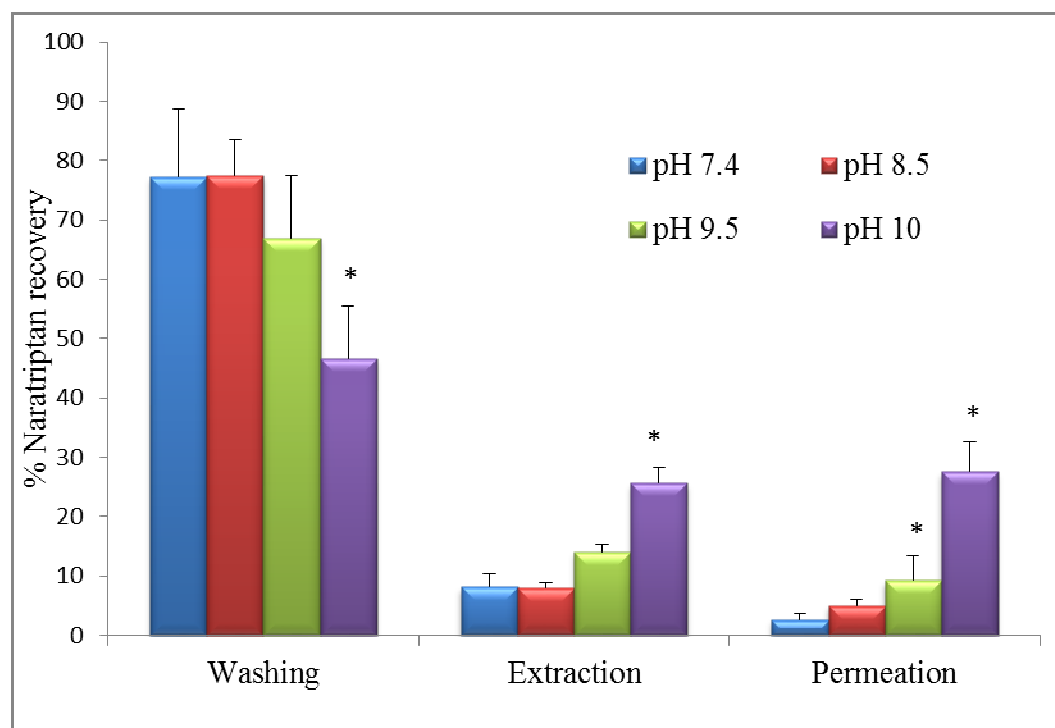


Figure 8. NAR mass balance studies for permeation studies of saturated drug in PBS for the pH range 7.4 – 10 (n=5, mean \pm SD); * denotes significant differences ($p < 0.05$)